

# Photostability of $D-\pi-A$ nonlinear optical chromophores containing a benzothiazolium acceptor

Marek Cigáň<sup>a\*</sup>, Anton Gáplovský<sup>a</sup>, Ivica Sigmundová<sup>b</sup>, Pavol Zahradník<sup>b</sup>, Roman Dědic<sup>c</sup> and Magdaléna Hromadová<sup>d</sup>



For the practical application of second-order NLO materials, not only a high molecular quadratic hyperpolarizability  $\beta$  but also good thermal, chemical, and photochemical stabilities are required. Most of the state-of-the-art chromophores with high NLO response cannot be put to use because they are photochemically highly unstable. Good thermal and photochemical stabilities with preserved high hyperpolarizabilities can be achieved by replacement of an aromatic ring with easily delocalizable heteroaromatics, e.g., with benzothiazole. Furthermore, desirable modifications of the benzothiazole fragment lead to improvement in  $\beta$  values. Here we report results of a comprehensive investigation of the photochemical stability of seven  $D-\pi-A$  push-pull molecules based on a  $N$ -methylbenzothiazolium acceptor and a  $N,N$ -dimethylaminophenyl donor with a different length of conjugated bridge and different acceptor strength. The quantum yield ( $\Phi$ ) and the kinetic parameters of photoreactions were determined for existing photodegradation pathways on irradiation at 300–850 nm in MeOH. *Trans-cis* photoisomerization is proposed as a fast but inefficient photobleaching mechanism for these irradiation wavelengths. Self-sensitized photooxidation by  $^1O_2$  makes very slow parallel photodegradation pathway and, albeit to small value of  $\Phi$ , plays a dominant role in the photodegradation of the compounds investigated. Both structural modifications (extension of conjugated bridge and an additional acceptor group bonded to heterocycle) resulting in an increase of NLO response led to a decrease in photostability due to the self-sensitized  $^1O_2$  photooxidative attack. Thus a compromise should be found between an increase in NLO response and a decrease in photostability to make a choice of studied compounds for practical applications. Copyright © 2010 John Wiley & Sons, Ltd.

Supporting information may be found in the online version of this paper.

**Keywords:** benzothiazolium  $D-\pi-A$  NLO chromophores; photooxidation; photostability; singlet oxygen; *trans-cis* photoisomerization

## INTRODUCTION

In the past fifteen years, a considerable effort has been focused on the development of organic molecules with enhanced second order nonlinear optical (NLO) properties due to their potential applications in various areas such as optical modulation, frequency doubling and molecular switching.<sup>[1–5]</sup> The most widely studied second-order (quadratic) NLO effects such as second harmonic generation (SHG) arise from high first molecular hyperpolarizabilities  $\beta$ . The most common design of molecules with large  $\beta$  values comprises strong electron donors and acceptors connected by a  $\pi$ -conjugated system (donor- $\pi$ -acceptor or 'push-pull' chromophores).<sup>[1,2]</sup> In such donor- $\pi$ -acceptor ( $D-\pi-A$ ) systems, the donor and acceptor moieties provide the necessity of ground-state charge asymmetry, whereas the  $\pi$ -conjugated bridge provides a pathway for the redistribution of electron density under the influence of external electric fields.<sup>[6]</sup>

For the practical application of second-order NLO materials, not only a high molecular quadratic hyperpolarizability  $\beta$ , but also good thermal, chemical and photochemical stabilities are required.<sup>[7,8]</sup> Good thermal and photochemical stabilities of NLO chromophores with preserved high hyperpolarizabilities can be achieved by replacement of an aromatic ring with easily delocalizable heteroaromatics.<sup>[9]</sup> In respect of these findings,

benzothiazole-derived dyes with a  $D-\pi-A$  setup were found to be promising candidates for NLO applications.<sup>[10]</sup> Further improvement in  $\beta$  values was achieved by proper introduction of donor and acceptor substituents onto the benzothiazole core due to its nonsymmetric character and quaternization of the benzothiazole nitrogen.<sup>[11]</sup> Benzothiazolium styryl dye and its derivatives with different donors and acceptors were widely investigated in last

\* Correspondence to: M. Cigáň, Institute of Chemistry, Faculty of Natural Sciences, Comenius University, SK-842 15 Bratislava, Slovakia.  
E-mail: cigan@fns.uniba.sk

a M. Cigáň, A. Gáplovský  
Institute of Chemistry, Faculty of Natural Sciences, Comenius University, SK-842 15 Bratislava, Slovakia

b I. Sigmundová, P. Zahradník  
Department of Organic Chemistry, Faculty of Natural Sciences, Comenius University, SK-842 15 Bratislava, Slovakia

c R. Dědic  
Department of Chemical Physics and Optics, Faculty of Mathematics and Physics, Charles University Prague, CZ-12116 Prague, Czech Republic

d M. Hromadová  
Department of Molecular Electrochemistry, J. Heyrovský Institute of Physical Chemistry of ASCR, v.v.i, CZ-182 23 Prague, Czech Republic

century as good laser<sup>[12]</sup> and NLO dyes.<sup>[13]</sup> Over the last few years, our research group synthesized a large number of push-pull 3-alkyl-benzothiazolium salts with different number  $n$  of ethylene units in a  $\pi$ -conjugated bridge and various donor and acceptor substituents.<sup>[11,14–17]</sup> The benzothiazolium salts were found to be much more effective NLO-phores in comparison with the corresponding neutral benzothiazoles. It was shown that the length of the  $\pi$ -conjugated bridge between the electron-donating group and benzothiazolium moiety, as well as the donor and acceptor ability, have a significant influence on  $\beta$ . Recently, Coe *et al.*<sup>[18]</sup> reported the results of Hyper-Rayleigh scattering (HRS) measurements for 3-methyl-benzothiazolium salts ( $n = 1–4$ ;  $D = N,N$ -dimethylaminophenyl) in comparison with the analogous 1-methylpyridinium salts. Experimental measurements revealed that the static molecular quadratic hyperpolarizability  $\beta_0$  increases with the length of polyene chain, and the benzothiazolium salts exhibit larger NLO responses than their pyridinium analogues.

In most cases, donors and acceptors in  $D-\pi-A$  systems are connected via the conjugated bridge containing C=C bonds. However, this bond readily undergoes *trans-cis* photoisomerization, which may hamper the material efficiency and lifetime. It was previously reported that the primary causes of photochemical instability of NLO chromophores containing C=C bonds are photooxidation and photoisomerization.<sup>[19–24]</sup> In either case, the nonlinear activity is significantly diminished, the charge-transfer (CT) system is reduced, and new absorption features appear elsewhere in the spectrum, usually at a much shorter wavelength. The identity and the number of specific reactions and their relative rates are influenced in a complicated way by the exact identity of the chromophore, the influence of atmospheric environment, the irradiation wavelength, the temperature, etc. Photostability of organic dyes is consequently often considered the Achilles Heel of organic photonic materials<sup>[8,20,25,26]</sup> and limits their practical applications. Most of the state-of-the-art chromophores which were designed to have high electro-optic coefficients and hyperpolarizabilities cannot be put to use because they are highly unstable and degrade because of a photochemically generated singlet oxygen.<sup>[8,27]</sup>

Here we report results of a comprehensive investigation of the photochemical stability, particularly the photooxidative stability of seven benzothiazolium iodides with a different length of conjugated bridge and a different acceptor strength of benzothiazolium core caused by withdrawing substituents. The studied compounds **1–7** are dipolar push-pull chromophores containing an  $N$ -methylbenzothiazolium electron-acceptor group, an alkenylene conjugation spacer with 1–3 double bonds and an  $N,N$ -dimethylamino group as a donor in the *para* position of the substituted phenyl group. The acceptor strength of **4–7** is enhanced by introducing an additional withdrawing substituent into the benzothiazole fragment ( $\text{NO}_2$  or  $\text{CN}$ ). The chemical structure of the compounds studied is presented in Fig. 1.

Experiments were carried out to determine the role of photoisomerization and photooxidation in the photodegradation of **1–7** and to evaluate the overall stability and availability of such molecules for practical applications.

## EXPERIMENTAL

### Synthesis

The compounds under study have been prepared by the condensation reactions as is presented in Fig. S1 (Supplementary

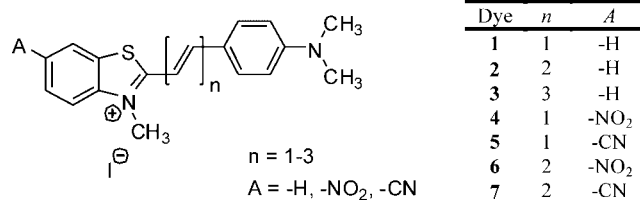


**Figure 1.** Chemical structure of the studied  $D-\pi-A$  benzothiazolium salts

Material) and has been published in Ref. <sup>[11]</sup>. The pyridine or piperidine have been used as the base. All compounds have all-*trans* configuration of double bonds in the conjugated bridge.

### Experimental techniques

Electronic absorption spectra were obtained on a Hewlett Packard HP 8452A diode array spectrophotometer and fluorescence measurements were performed on a Hitachi F-2000 fluorescence spectrophotometer. The solvent used in all measurements was methanol (MeOH) because of the good solubility of the compounds investigated and the good photostability of 2,5-dimethylfuran (2,5-DMF) and 2,5-diphenylisobenzofuran (DPIBF) as actinometric indicators of photooxidative attack of singlet oxygen ( $^1\text{O}_2$ ) in this solvent (Sections 2 and 3 in Experimental). All photodegradation measurements were carried out at 25 °C in the dark with only the 100-W xenon lamp as the light source. Concentrations of **1–7** never exceeded  $2 \times 10^{-5} \text{ mol dm}^{-3}$ , to avoid molecule aggregation and photochemical dimerization processes.

### Photodegradation measurements

All photochemical measurements were performed using the apparatus described elsewhere (Fig. 7 without ultrasonic horn H).<sup>[28]</sup> The light source was a 100-W xenon lamp (300–850 nm;  $I_0 = 2.05 \pm 0.05 \times 10^{-5} \text{ mol s}^{-1} \text{ dm}^{-3}$ ). The actual concentration of compounds studied in air-saturated solutions during irradiation was measured spectrophotometrically (HP 8452A) at shielding the incident photon flux from the light source. Absorbed photon flux  $I_a$  (by compound X) was calculated from emission curves for the light source measured on an Ocean Optics SD 2000 spectrophotometer using the following equation:

$$I_a = I_0 - I_T = I_0 \int_0^\infty \left( 1 - 10^{-\sum_i A_{\lambda i}} \right) \frac{A_{\lambda X}}{\sum_i A_{\lambda i}} \frac{I_\lambda}{\int_0^\infty I_\lambda d\lambda} d\lambda$$

$$= I_0 \frac{\int_\lambda S_0 d\lambda - \int_\lambda S_T d\lambda}{\int_\lambda S_0 d\lambda}, \quad (1)$$

where  $\int S_0 d\lambda$  and  $\int S_T d\lambda$  denote the total area under the emission spectrum of the light source after passing through a cuvette without and with X, respectively,  $I_0$  and  $I_T$  the incident and the transmitted photon flux, respectively,  $A$  means absorbance (the value of absorbed photon flux during photodegradation depends on time – for detailed calculation of  $\Phi$  during photodegradation of studied compounds using time-dependent values of  $I_a$  refer Eqns (7) and (10)). The incident photon flux  $I_0$  in all measurements was determined using the integrated form of the equation for

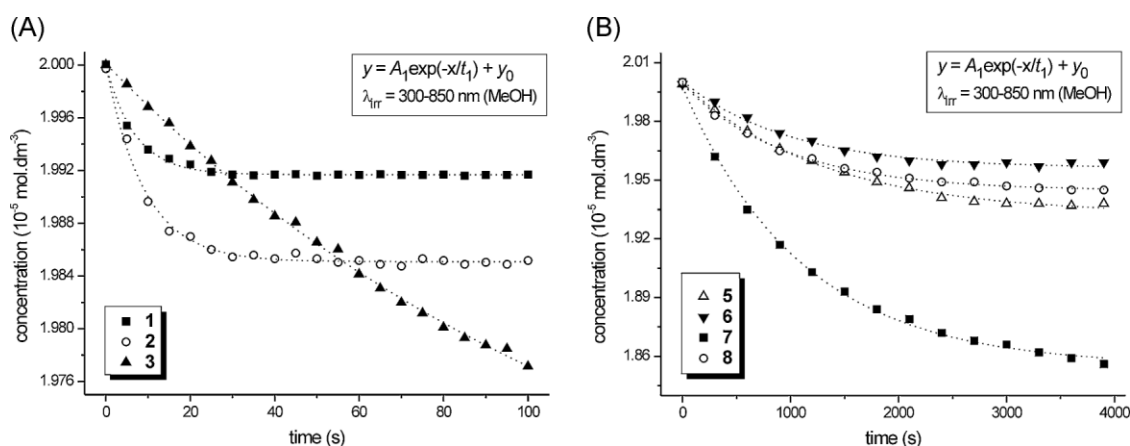


**Figure 2.** Changes in the concentrations of 1–3 (A) and 4–7 (B) in MeOH on irradiation with a 100-W Xe lamp (300–850 nm;  $I_0 = 2.05 \pm 0.05 \times 10^{-5} \text{ mol s}^{-1} \text{ dm}^{-3}$ ). Time-dependent concentrations are fitted by single exponential functions [dotted line]

$\Phi^1\text{O}_2$  determination for a solution of a sensitizer with known  $\Phi^1\text{O}_2$  and an acceptor with known  $\beta$  (Eqn (5)).

#### Determination of singlet oxygen quenching rate constants ( $k_Q$ )

The rate constant  $k_Q$  for  $^1\text{O}_2$  quenching (relative reactivity index  $\beta_Q = k_d/k_Q$ ; in this case  $\beta_Q$  includes both physical and chemical quenching) by 1–7 necessary for more accurate  $\Phi^1\text{O}_2$  determination were calculated based on inhibition of DPIBF oxidation ( $\beta = 1.1 \times 10^{-4} \text{ M}$  in MeOH<sup>[29,30]</sup>) by competitive  $^1\text{O}_2$  quenching<sup>[31,32]</sup> using the following equations (in the primary model we replaced the concentrations with the corresponding absorbances):

$$k_Q = \frac{k_r([A_{\text{DPIBF}}/\varepsilon_{\text{DPIBF}}]_t^Q - [A_{\text{DPIBF}}/\varepsilon_{\text{DPIBF}}]_t^0) + k_d \ln([A_{\text{DPIBF}}]_t^Q/[A_{\text{DPIBF}}]_t^0)}{[Q] \ln([A_{\text{DPIBF}}]_0/[A_{\text{DPIBF}}]_t^Q)} \quad (2)$$

$$\text{or } k_Q = \frac{k_d + k_r[\text{DPIBF}]_0}{[Q]} \left[ \frac{-\left(\frac{d[A_{\text{DPIBF}}/\varepsilon_{\text{DPIBF}}]}{dt}\right)^0}{-\left(\frac{d[A_{\text{DPIBF}}/\varepsilon_{\text{DPIBF}}]}{dt}\right)} - 1 \right], \quad (3)$$

and by monitoring the decrease of the DPIBF absorption band at different quencher concentration using Young's kinetic technique.<sup>[33]</sup>

$$S_0/S = 1 + k_Q/k_d[Q] = 1 + 1/\beta_Q[Q]. \quad (4)$$

Superscripts 0 and Q denote the absence and presence of quencher Q,  $[\text{DPIBF}]_0$  is the initial concentration of DPIBF,  $[Q]$  is the quencher concentration and  $S$  is the slope of the plot of a first-order disappearance of DPIBF at a given  $[Q]$ . Both methods were used to eliminate errors for time-dependent absorption measurements.  $^1\text{O}_2$  was generated by MB sensitization ( $\Phi^1\text{O}_{2(\text{MB})} = 0.50 \pm 0.01$  in MeOH<sup>[29,34]</sup>).

#### Determination of the quantum yield of singlet oxygen production ( $\Phi^1\text{O}_2$ )

Values of  $\Phi^1\text{O}_2$  were determined using an equation that describes the change in concentration  $c_A$  ( $\text{mol dm}^{-3}$ ) of a singlet oxygen acceptor (with known  $\beta$  value) after irradiation for a given time  $t$  (s) in the presence of a singlet oxygen generator (sensitizer

1–7) that absorbs a photon flux  $I_a$  ( $\text{mol s}^{-1} \text{ dm}^{-3}$ ) (Fig. 3).<sup>[34,35]</sup>

$$\begin{aligned} -\frac{dc_A}{dt} &= -\frac{d[\text{DMF}]}{dt} = I_a \Phi^1\text{O}_2(X) \frac{k_{\text{DMF}}^r[\text{DMF}]}{k_d + k_{\text{DMF}}^r[\text{DMF}] + k_{\text{Q}(X)}[X]} \\ &= \frac{[\text{DMF}]}{Z + [\text{DMF}]}, \quad Z = \beta + \frac{k_{\text{Q}(X)}[X]}{k_{\text{DMF}}^r}. \end{aligned} \quad (5)$$

In this approach, we involved quenching of  $^1\text{O}_2$  by a sensitizer using parameter  $Z$ . Parameter  $Z$  is the sum of two components and includes overall (physical and chemical) quenching of  $^1\text{O}_2$  by acceptor A (2,5-DMF;  $k_r = 3.9 \cdot 10^8 \text{ dm}^{-3} \text{ mol}^{-1} \text{ s}^{-1}$ <sup>[34]</sup>) and sensitizer X, and should be used for every sensitizer with high value of  $k_Q$  (e.g., omitting the parameter  $Z$  for sensitizer 3 with high value of  $k_Q$  leads to a reduction in quantum yield of about 60%). Parameter  $\beta$  is the reactivity index of the acceptor (the ratio between the rate constants for nonradiative unimolecular decay of  $^1\text{O}_2$  for the appropriate solvent  $k_d$  and acceptor oxidation  $k_r$ ).<sup>[36]</sup> Its value represents the acceptor concentration at which half the reactive  $^1\text{O}_2$  species will be trapped. Constant  $k_Q$  is the overall quenching constant for sensitizer X. Integrating the Eqn (5) and deducing acceptor concentrations from absorbance values gives:

$$A_a + \varepsilon_{\text{DMF}} Z \ln A_a = A_{a0} + \varepsilon_{\text{DMF}} Z \ln A_{a0} - I_a \varepsilon_{\text{DMF}} \Phi^1\text{O}_2(X) t, \quad (6)$$

where  $A_{a0}$  and  $A_a$  are the acceptor absorbance (e.g., at the position of maximum absorption) before and at various irradiation times,  $l$  is the optical path length (cm) and  $\varepsilon$  is the molar extinction coefficient of the acceptor. The slope of a plot of this equation against irradiation time gives  $\Phi^1\text{O}_2$  when the other parameters are known.

#### Superoxide anion ( $\text{O}_2^-$ ) detection by EPR

Electron paramagnetic resonance (EPR) spectra were recorded on an ERS 230 instrument (ZWG Berlin, Germany), which operates in the X-band ( $\sim 9.3 \text{ GHz}$ ) with a modulation amplitude of 0.1 mT and microwave power of 5 mW. A sample containing  $2.5 \times 10^{-5} \text{ mol dm}^{-3}$  of one of the derivatives studied was continuously irradiated at  $\sim 60 \text{ W m}^{-2}$  by a 250-W halogen lamp through a 10-cm water filter for 20 min. The superoxide anion radical generated was

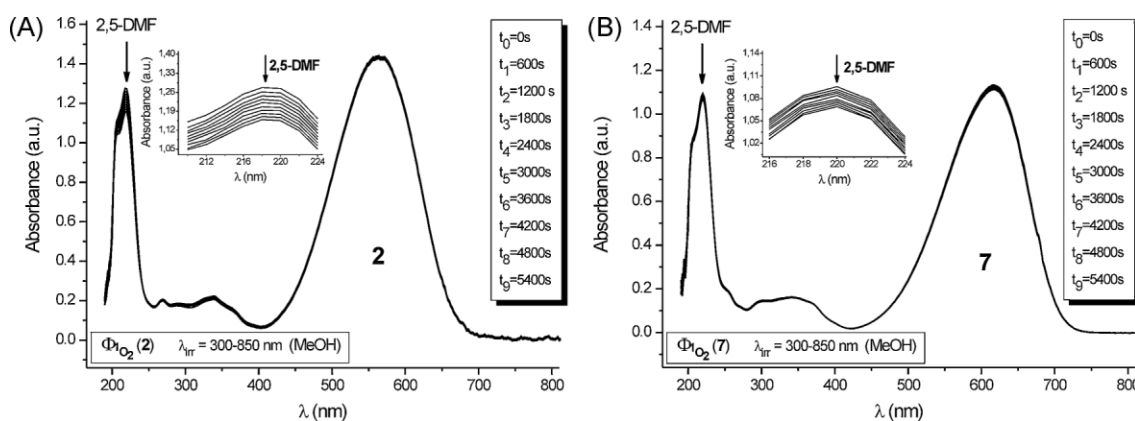


**Figure 3.** Kinetic changes in the absorption spectra of 2,5-DMF in MeOH during irradiation of **2** (A) and **7** (B) at 300–850 nm ( $I_0 = 2.05 \pm 0.05 \times 10^{-5} \text{ mol s}^{-1} \text{ dm}^{-3}$ ). Absorbed photon flux at  $t = 0 \text{ s}$  was  $I_{a0} = 1.38 \times 10^{-5} \text{ mol s}^{-1} \text{ dm}^{-3}$  for **2** and  $I_{a0} = 1.05 \times 10^{-5} \text{ mol s}^{-1} \text{ dm}^{-3}$  for **7**

indirectly monitored using a spin trap with 5,5-dimethyl-4,5-dihydroxypyrrole-*N*-oxide (DMPO, Sigma;  $c \sim 3.5 \times 10^{-4} \text{ mol dm}^{-3}$ ).<sup>[37,38]</sup>

#### Phosphorescence measurements (determination of the energy of a triplet state $E_T$ )

Phosphorescence spectra were detected using a home-built set-up for detection of weak near-IR luminescence described in Ref. <sup>[39]</sup>. Excitation pulses of  $\sim 10 \mu\text{J}$  and 4.5 ns wide were provided by the dye laser Lambda Physik FL1000 pumped by the excimer laser ATL Lasertechnik ATLEX 500i. The excitation wavelengths and laser dyes were chosen to match different absorption spectra of the investigated molecules, namely 524 nm (Coumarin 307), 540 nm (Coumarin 153), and 575 nm (Rhodamin 6G). The samples were excited through optically polished bottoms of fluorescence cells. Luminescence was collected by lens assembly through two long-pass filters Schott RG7 and high-luminosity monochromator Jobin Yvon H20IR to the infrared-sensitive photomultiplier Hamamatsu R5509 cooled to  $-50^\circ \text{C}$  by liquid nitrogen. The pulses from the photomultiplier were fed through the Becker–Hickl HF AC-26dB preamplifier to the Becker–Hickl MSA 200 photon counter/multiscaler with time resolution of 5 ns per channel. The spectra were obtained as integrals of the counts in each of the kinetics at individual wavelengths in the spectral region from 750 to 1350 nm and corrected in respect to the spectral sensitivity of the detection set-up as well as to the equivalent absorbed energy. The kinetics were fitted by double exponential decays to obtain phosphorescence lifetimes.

#### Determination of oxidation potential ( $E^O$ )

Iodides **1–7** were metathesized to their corresponding hexafluorophosphate salts (due to interfering signal of  $\text{I}^-$  anion) by precipitation from the MeOH/MeCN/aqueous  $\text{KPF}_6$ . Electrochemical measurements were done in a three-electrode arrangement using a home-made fast rise-time potentiostat. The instrument was interfaced to a personal computer via an IEEE-interface card (PC-Lab, AdvanTech Model PCL-848) and a data acquisition card (PCL-818) using 12-bit precision. Positive iR compensation just short of oscillations was used in all the measurements. The reference electrode  $\text{Ag}|\text{AgCl}|1\text{M LiCl}$  was separated from the test solution by a salt bridge. The working electrode was a glassy

carbon electrode with an area of  $3.79 \times 10^{-3} \text{ cm}^2$ . The auxiliary electrode was a cylindrical platinum net. Ferrocene was used as an internal reference and all data are referred to the formal redox potential of the ferrocene/ferrocenium ( $\text{Fc}/\text{Fc}^+$ ) couple equal to  $+0.52 \text{ V}$  in this system. Oxygen was removed from the solution by a stream of argon, which blanketed the solution throughout the measurements.  $E^O$  values were obtained from the cyclic voltammetric measurements of 0.5 mM solutions of **1–7** in acetonitrile and 0.1 M tetrabutylammonium hexafluorophosphate supporting electrolyte. Error in the  $E^O$  determination is  $\pm 0.005 \text{ V}$ . Estimated values  $E^O$  for **1–3** agree well with the literature data.<sup>[18]</sup>

## RESULTS AND DISCUSSION

### Spectral characteristics

The UV–visible absorption spectra of salts **1–7** in MeOH were measured previously.<sup>[11]</sup> These spectra are dominated by intense low-energy bands in the visible region ( $\lambda_A$  520–630 nm) attributable to  $\pi \rightarrow \pi^*$  ICT transitions from the terminal electron-donating *N,N*-dimethyl groups to the central benzothiazolium skeleton. Less intense bands in the spectra are associated with nondirectional  $\pi \rightarrow \pi^*$  transitions at higher energy. Basic absorption characteristics of ICT transitions (absorption maxima  $\lambda_A$ , extinction coefficient  $\log \epsilon$ , oscillator strength  $f$ , ICT energies  $E_A$ ) and calculated values of first hyperpolarizabilities  $\beta$  (at the semiempirical PM3 level by the finite-field method)<sup>[11]</sup> of benzothiazolium NLO chromophores **1–7** are presented in Table 1. ICT bands move predictably to lower energy with increasing conjugation length and with increasing acceptor strength of the benzothiazolium skeleton. An additional acceptor group bound to the benzothiazolium ring ( $\text{NO}_2$  or  $\text{CN}$ ) has a controversial effect on the NLO response of **4–7**. Addition of this group to chromophore **1** with single double bond enhances the value of  $\beta$  and addition to chromophore **2** with two double bonds leads to a modest decrease in NLO response. A rising number of double bonds enhances the NLO response of benzothiazolium chromophores. Different equilibrium between benzenoid form and quinoid form(s) in the ground and the excited state together with possible isomerization in longer linkers<sup>[40]</sup> could explain the lowered values of  $\log \epsilon$ ; and  $f$  in absorption spectra of compound **6**.

**Table 1.** Photophysical properties of the molecules studied

Dye	$\lambda_A$ (nm)	$E_A$ (kJ mol <sup>-1</sup> )	log $\varepsilon$	$f$	$\lambda_P$ (nm)	$E_T$ (kJ mol <sup>-1</sup> )	$\tau_1$ (ns)	$\tau_2$ ( $\mu$ s)	$\beta$ (10 <sup>-30</sup> esu)
<b>1</b>	520	230	4.83	1.07	841	142	85 $\pm$ 3	1.3 $\pm$ 0.4	98.5
<b>2</b>	562	213	4.78	1.24	851	141	76 $\pm$ 4	1.2 $\pm$ 0.1	370.1
<b>3</b>	580	206	4.75	1.33	861	139	79 $\pm$ 8	1.4 $\pm$ 0.1	744.8
<b>4</b>	562	213	4.90	0.99	854	140	82 $\pm$ 9	1.2 $\pm$ 0.1	183.3
<b>5</b>	551	217	4.91	1.01	863	139	90 $\pm$ 8	1.2 $\pm$ 0.1	183.7
<b>6</b>	630	190	4.61	0.62	852	140	83 $\pm$ 1	1.2 $\pm$ 0.2	317.3
<b>7</b>	618	194	4.83	1.14	850	142	83 $\pm$ 2	1.1 $\pm$ 0.1	321.0

$\lambda_A$ , the absorption maximum; log  $\varepsilon$ , the extinction coefficient;  $f$ , the oscillator strength;  $E_A$ , the ICT energies;  $\lambda_P$ , the phosphorescence maximum;  $E_T$ , the energy of triplet state;  $\tau_1$  and  $\tau_2$ , fast and slow decay time of luminescence signals;  $\beta$ , the first hyperpolarizability.

Fluorescence spectra showed very low intensity in MeOH (quantum yields of fluorescence  $\Phi_F$  never exceeded 0.005). This can be attributed to enhanced ICT interaction, which often results in fluorescence quenching due to enhanced probability of nonluminescent ICT and TICT (twisted intramolecular charge transfer) state population in polar solvents.<sup>[41]</sup> The same effect was observed in a few push-pull *D*- $\pi$ -*A* salts and it has also a practical application.<sup>[42]</sup> The evidence of the final relaxed nonluminescent dark TICT state in the commercial benzothiazolium push-pull laser dye LDS 751 (which is structurally very close to dye **2**) was recently confirmed experimentally using the FS TR SEP FD method (femtosecond time resolved stimulated emission pumping fluorescence depletion).<sup>[43]</sup> Hydrogen bonding effect of the solvent can also contribute to the nonradiative internal conversion.<sup>[41]</sup>

Phosphorescence spectra were measured to estimate the energy of triplet states (the position of the main phosphorescence maxima  $\lambda_P$ , Table 1) as one of the major factors that influence the production and quenching of singlet oxygen <sup>1</sup>O<sub>2</sub> (Sections 2.2 and 2.3 in Results and Discussion). All the studied compounds exhibit similar luminescence spectra with  $\lambda_P$  around 852  $\pm$  11 nm and a shoulder around 910 nm. Bathochromic shift of the main phosphorescence maximum with the length of the conjugated bridge was observed for chromophores **1–3**. On the contrary, no such shift was found for compounds **4** and **6** and a hypsochromic shift was obtained for compounds **5** and **7**. Luminescence intensity exhibits very strong dependence on the length of the conjugated bridge and on addition of the acceptor to *N*-methylbenzothiazolium moiety. It increases significantly with increasing length of the conjugated bridge. This effect was the most pronounced in chromophores **1–3**, where compound **1** exhibited only approximately 3% of the total phosphorescence intensity of compound **2**, while the phosphorescence intensity of compound **3** was  $\sim$ 27 times higher than that of compound **2**. This effect was also observed in compounds **4** and **6** as well as in **5** and **7** where the total phosphorescence intensity increased 5 and 7 times, respectively, in the compounds with longer conjugated bridges. Similarly an addition of the acceptor to heterocycle significantly increases the luminescence intensity. Time-resolved luminescence signals were accurately fitted by biexponential functions. We distinguished fast ( $\tau_1$ ) and slow ( $\tau_2$ ) decay times of approximately 80  $\pm$  10 ns and 1.3  $\pm$  0.1  $\mu$ s, respectively, with the short component fractional yield of  $\sim$ 70–75% from the biexponential fits. The short component of the luminescence signal is assumed to result from a deactivation of the dark TICT state<sup>[43]</sup> or it may be as well a component of

phosphorescence. However, the second alternative is quite unusual for most organic triplets. All the respective lifetimes are quite similar, one can only say that longer component is always (for all different excitation wavelengths) slower in sample **3** (refer Table 1). The striking differences in phosphorescence intensities of the different materials are therefore caused by different triplet state quantum yields and not by different quenching of the emitting states. Thus, the extension of the conjugated bridge and an additional acceptor group bonded to the heterocycle have a substantial effect on the triplet state population although they do not significantly influence the energy of the triplet states.

### Photostability

As already mentioned, the NLO chromophores photostability is a very important characteristic with regard to their practical usage. There are two dominant processes leading to photodegradation of NLO chromophores containing a carbon-carbon double bond as part of a  $\pi$ -conjugated bridge: *trans*-*cis* isomerization and photooxidation. To study the influence of the extension of the conjugated bridge and the addition of an acceptor group to the heterocycle on the photostability of **1–7**, MeOH solutions of the compounds were subjected to irradiation with a 100-W Xe lamp.

#### *Trans*-*cis* photoisomerization

Changes in the main absorption band (ICT transition) were monitored to determine the photodegradation quantum yield in air-saturated MeOH solutions under one-photon excitation at room temperature. Kinetic changes in the absorption spectra of **1–7** in MeOH on irradiation at 300–850 nm are presented in Figs. S2 (Supplementary Material) and 2. The main absorption during this irradiation corresponds to ICT transitions for all compounds studied. In all cases, the ICT absorption band initially decreased with irradiation time and the absorption bands were shifted to a shorter wavelength. After longer irradiation, a photostationary state was attained and the spectra of the reaction mixtures did not change with further irradiation (small concentration changes due to self-sensitized <sup>1</sup>O<sub>2</sub> photooxidative attack were not detectable in such short time intervals). These results can be rationalized by the existence of *trans*-*cis* photoisomerization, leading to a photostationary state. The data was fitted to a monoexponential decay function and the decay rate constants determined from the fitted curves were used to calculate the quantum yield of photodegradation (i.e., photoisomerization)

**Table 2.** Photodegradation characteristics of **1–7** on irradiation at 300–850 nm

Dye	$k$ ( $10^{-4} \text{ s}^{-1}$ )	$t_{0.5}$ (min)	$t_{0.9}$ (min)	$\Phi_{\text{deg}} \times 10^{-4}$	% initial	% $^1\text{O}_2$ contribution
<b>1</b>	1800	0.07	0.22	4.33	99.6	0.002
<b>2</b>	1150	0.10	0.33	5.60	99.2	0.060
<b>3</b>	76.0	1.52	5.05	0.57	97.9	2.2
<b>4</b>	7.8	15	49	0.15	96.7	3.2
<b>5</b>	10.0	12	38	0.13	97.9	1.4
<b>6</b>	9.1	13	42	0.66	92.8	0.6
<b>7</b>	10.0	12	38	0.18	97.2	1.5

$k$ , the photodegradation rate constant;  $t_{0.5}$ , the time for 50% degradation;  $t_{0.9}$ , the time for 90% degradation;  $\Phi_{\text{deg}}$ , the quantum yield for photodecomposition; % initial, the percent of initial isomer in the photostationary state; %  $^1\text{O}_2$  contribution, the contribution of self-sensitized photooxidation by  $^1\text{O}_2$  to overall photodegradation during photoisomerization.

according to:

$$\Phi_{\text{deg}} = \frac{-\int_{c_0}^{c_t} dc}{\int_0^t I_a dt} = \frac{c_0 - c_t}{\frac{t_{0.9}}{n+1} \sum_{i=0}^n \frac{I_{a_i} + I_{a_{i+1}}}{2}} = \frac{c_0 - c_t}{\left(\frac{I_{a0} + I_{a0.9}}{2}\right) t_{0.9}}, \quad t_{0.9} = \frac{\ln 10}{k} \quad (7)$$

Values for the photodegradation rate constant ( $k$ ), the time for 50% degradation ( $t_{0.5}$ ), the time for 90% degradation ( $t_{0.9}$ ), the quantum yield for photodecomposition ( $\Phi_{\text{deg}}$ ), the percent of initial isomer in the photostationary state and the contribution of self-sensitized photooxidation by  $^1\text{O}_2$  to overall photodegradation during photoisomerization are summarized in Table 2.

$\Phi_{\text{deg}}$  exhibited no concentration dependence, consistent with a first-order photodecomposition process. The values of  $\Phi_{\text{deg}}$  ranged from  $(0.11\text{--}0.14) \times 10^{-4}$  (2% photodegradation) for **5** to  $(5.5\text{--}5.7) \times 10^{-4}$  (0.8% photodegradation) for **2**, with the percentage photodegradation calculated from the asymptotes of the fitted exponential curves. Small values of  $\Phi_{\text{deg}}$  are most likely connected with the extent of CT character in the molecules studied. Substantial competition of the ICT (and/or TICT) excited-states population with the nonradiative phantom-state population (from the second one *trans-cis* isomerization occurs) and moreover the hydrogen bonding effect of MeOH may enhance the nonradiative internal conversion.<sup>[41]</sup> Addition of the third double bond to the conjugated bridge and an additional acceptor bound to position 6- of *N*-methylbenzothiazolium decreased the value of  $\Phi_{\text{deg}}$ , although the overall percentage photodegradation slightly increased. Very rapid *cis-trans* photoisomerization of the initially formed *cis* isomer may be responsible for a low contribution of this pathway to the overall photodegradation. *Trans-cis* photoisomerization thus seems to be a fast (mainly for **1–3**) but inefficient ( $\sim 1\text{--}7\%$  decrease of initial concentration) photobleaching mechanism for these irradiation wavelengths. Contribution of self-sensitized photooxidation by  $^1\text{O}_2$  (Section 2.4 in Results and Discussion) as a parallel degradation pathway to the overall photodecomposition during *trans-cis* photoisomerization of **1–7** is not significant (0–3%).

#### Photooxidation

There are two possible mechanisms for interaction between an excited dye molecule and dioxygen, which lead to the formation of singlet oxygen (Type II process) and a superoxide anion (Type I

process), respectively, both of which can contribute to dye photofading.<sup>[44,45]</sup> Therefore, we conducted experiments to determine whether **1–7** generate these reactive oxygen species and whether there is evidence of self-sensitized photooxidation.

**Production of the superoxide anion radical  $\text{O}_2^-$ .** To study the generation of superoxide anion radical  $\text{O}_2^-$  after photoexcitation of **1–7**, EPR spin-trapping was carried out with DMPO as the spin trapper.<sup>[34,35]</sup> After 20 min of irradiation with a 250-W halogen lamp only **4** showed a very low-intensity EPR signal (Fig. S3 in Supplementary Material) in the region of free radicals ( $g = 2.004$ ). This signal seemed to represent DMPO- $\text{O}_2^-$  adduct with three coupling constants due to the nitrogen atom and two hydrogen atoms in the  $\beta$  and  $\gamma$  positions in this molecule ( $A_N = 13.3 \text{ G}$ ,  $A_H^\alpha = 10.1 \text{ G}$  and  $A_H^\beta = 1.5 \text{ G}$ ). Experimental coupling constants agree well with literature data.<sup>[37,38]</sup> Electron transfer (formation of a superoxide anion radical) and subsequent oxidation reactions (followed by various radical recombinations) or nucleophilic addition of  $\text{O}_2^-$  thus may contribute to the overall degradation of **4**.

**Production of singlet oxygen  $^1\text{O}_2$ .** Values for the quantum yield of singlet oxygen production ( $\Phi^1\text{O}_2$ ) are summarized in Table 4 and outlined in Fig. 3. Relatively low values of  $\Phi^1\text{O}_2$  for all seven derivatives can be attributed to the ICT character of these molecules, which manifests its effect in sensitizer–oxygen contact complexes.<sup>[46,47]</sup> CT character in the sensitizer can influence the energy, yield, and lifetime of the triplet state, all of which can, likewise, ultimately be reflected in the singlet oxygen yield. Increasing CT interactions reduce the overall quantum yield of singlet oxygen formation  $\Phi^1\text{O}_2$  and the decrease is further enhanced in polar solvents due to the enhancement of CT interactions (stabilization of exciplexes of triplet excited sensitizer and  $\text{O}_2$  in moving from nonpolar to highly polar solvents). The extent of CT, both within the sensitizer itself (i.e., intramolecular CT) as well as in the sensitizer–oxygen complex (i.e., intermolecular CT), thus have a large adverse effect on the efficiency with which singlet oxygen is generated.<sup>[48]</sup>

The increasing value of  $\Phi^1\text{O}_2$  after addition of the acceptor groups to the *N*-methylbenzothiazolium moiety of **1** (simultaneous increase of  $E^0$ ) demonstrates an effect of intermolecular CT (molecules **4** and **5**). This behavior does not take effect on going from molecule **2** to structure **6** and **7** and even a slight decrease of  $\Phi^1\text{O}_2$  in both cases was observed. These results

**Table 3.** Parameters for characterization of physical and chemical quenching of  $^1\text{O}_2$  by **1–7**

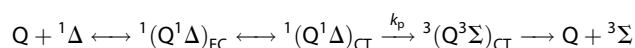
Dye	$k_Q$ ( $10^9 \text{ dm}^3 \text{ mol}^{-1} \text{ s}^{-1}$ )	$\beta_Q$ ( $10^{-5} \text{ mol dm}^{-3}$ )	$E^0$ vs. $Fc/Fc^+$ (V)	$\mu$ (D)	$k_r$ ( $10^6 \text{ dm}^3 \text{ mol}^{-1} \text{ s}^{-1}$ )	$\beta_r$ ( $10^{-2} \text{ mol dm}^{-3}$ )
<b>1</b>	0.17	65.0	0.567	2.4	$\leq 0.1$	$\geq 10$
<b>2</b>	1.50	7.3	0.381	4.1	$\leq 0.1$	$\geq 10$
<b>3</b>	5.00	2.2	0.264	7.3	$\leq 0.1$	$\geq 10$
<b>4</b>	1.20	9.2	0.626	12.4	3.2	3.5
<b>5</b>	0.41	26.8	0.610	7.3	1.5	7.5
<b>6</b>	3.70	3.0	0.435	12.0	2.2	5.0
<b>7</b>	7.10	1.6	0.424	6.1	1.5	7.3

$k_Q$ , the rate constant for overall  $^1\text{O}_2$  quenching;  $\beta_Q$ , the relative reactivity index (includes both physical and chemical quenching) for  $^1\text{O}_2$  quenching;  $E^0$ , the formal redox potential;  $\mu$ , the ground-state dipole moment;  $k_r$ , the rate constant for  $^1\text{O}_2$  photooxidative attack;  $\beta_r$ , the reactivity index of dye with  $^1\text{O}_2$ .

suggest a controversial role of a combination of both inter- and intramolecular CT on the  $^1\text{O}_2$  production efficiency, possibly affecting the quantum yield of the triplet state population and/or a triplet state deactivation pattern. As was previously mentioned by Nielsen *et al.*,<sup>[48]</sup> one cannot always rely on rule-of-thumb guidelines when attempting to construct either efficient or inefficient  $^1\text{O}_2$  sensitizers and a full investigation of the photophysical properties of the system studied is generally required.

The value of  $\Phi^1\text{O}_2$  for **1–3** represents again an unexpected decrease of  $\Phi^1\text{O}_2$  of **1–3** with increasing value of  $E_0$ . This increasing tendency of a quantum yield with extension of conjugated bridge copies the ability of phosphorescence emission by molecules **1–3** although only qualitative conclusions of the emission probability could be done. This behavior is consistent with the fact that the  $S_0$ – $S_1$  excitation energy changes more with the conjugate chain length than that of  $S_0$ – $T_1$ .<sup>[49,50]</sup> Enhancement in rate constants for intersystem crossing for longer chains was observed and attributed to a lowering of the  $S_1$ – $T_1$  energy gap for longer chains.<sup>[49,51]</sup> Thus, molecules with longer conjugation lengths seem to have a higher triplet quantum yield. The first excited singlet states of **1–7** should not contribute markedly to overall  $^1\text{O}_2$  production owing to their short lifetimes  $\tau_0 \leq 10 \text{ ns}$  ( $\tau_0 = 1.5/\nu_{\text{max}}^2$  where  $\nu_{\text{max}}$  is the wavenumber corresponding to the absorption maximum). The  $^1\text{O}_2$  production efficiency of the studied molecules is clearly the greatest for **3** and the least for **1**.

**Quenching of singlet oxygen.** Estimated values of  $^1\text{O}_2$  quenching rate constants  $k_Q$  ( $\beta_Q$ ) (Table 3) exceeded the values expected for an electronic-to-vibrational energy transfer (converting electronic excitation energy of the  $^1\text{O}_2$  molecule into vibration of  $\text{O}_2$  and quencher Q) by orders of magnitude. These high values of  $k_Q$  regarding relatively high triplet energies ( $E_T > 130 \text{ kJ mol}^{-1}$ ) and low oxidation potentials ( $E^0 < 0.65 \text{ V}$ ) can be attributed to a CT-induced quenching of  $^1\text{O}_2$ , where the deactivation of the initially formed singlet encounter complex  $^1(\text{Q}^1\Delta)_{\text{EC}}$  is enhanced by the formation of a singlet exciplex  $^1(\text{Q}^1\Delta)_{\text{CT}}$ , which is stabilized by the transfer of electric charge from the quencher to the oxygen molecule.<sup>[52]</sup> Iodides do not contribute significantly to such high  $k_Q$  values in protic solvents.<sup>[53]</sup> The formation of a singlet exciplex  $^1(\text{Q}^1\Delta)_{\text{CT}}$  is followed by isc to the ground-state CT complex, by chemical reaction, or by separation of free ions. Thus, the overall quenching rate constant  $k_Q$  can be additively composed of a physical and a chemical component, i.e.,  $k_Q = k_p + k_r$ .



Rate constants  $k_Q$  of **1–7** showed very strong dependence on the length of the conjugated bridge and an addition of acceptor group to the *N*-methylbenzothiazolium moiety. Values of  $k_Q$  increased significantly with both characteristics. Both quenching

**Table 4.** Parameters for characterization of  $^1\text{O}_2$  production by **1–7** and subsequent self-sensitized photooxidation

Dye	$\Phi^1\text{O}_2$	$E^0$ vs. $Fc/Fc^+$ (V)	$t_{1/2(1\text{O}_2)}$ (days)	$t_{9/10(1\text{O}_2)}$ (days)	$\Phi_{r(1\text{O}_2)}$
<b>1</b>	0.0006	0.567	80.5	362	$0.0063 \times [\text{C}]$
<b>2</b>	0.0014	0.381	29.5	124	$0.014 \times [\text{C}]$
<b>3</b>	0.0098	0.264	4.1	15	$0.098 \times [\text{C}]$
<b>4</b>	0.0012	0.626	13.5	60	$0.034 \times [\text{C}]$
<b>5</b>	0.0009	0.610	38.8	177	$0.012 \times [\text{C}]$
<b>6</b>	0.0011	0.435	25.0	115	$0.021 \times [\text{C}]$
<b>7</b>	0.0012	0.424	27.0	116	$0.017 \times [\text{C}]$

$\Phi^1\text{O}_2$ , the quantum yield of  $^1\text{O}_2$  production;  $E^0$ , the formal redox potential;  $t_{1/2(1\text{O}_2)}$  and  $t_{9/10(1\text{O}_2)}$ , the half-life time of the self-sensitized photooxygenation reaction and the time of degradation of 90% of the compound at these reaction;  $\Phi_{r(1\text{O}_2)}$ , the quantum yield of the self-sensitized photodegradation by  $^1\text{O}_2$ .

of  $^1\text{O}_2$  and  $^1\text{O}_2$  production depends on two main parameters: triplet-state energy  $E_T$  and oxidation potential of the sensitizer. The oxidation process is reversible for all studied compounds and its formal redox potential  $E^{\circ}$  is reported in Table 3. Because of the almost constant value of  $E_T$ , increasing  $k_Q$  with extension of the conjugated bridge can be rationalized by the decreasing value of  $E^{\circ}$ . This is an established phenomenon.<sup>[52]</sup> Albeit to the opposite effect of  $\text{NO}_2$  (CN) group addition on  $E^{\circ}$ ,  $k_Q$  considerably increased after incorporation of these groups to the benzothiazolium moiety. Considering again the relatively constant values of  $E_T$ , these results indicate a significant role of intramolecular charge-transfer (ICT) in the CT-induced quenching of  $^1\text{O}_2$ . ICT most likely plays an important role not only in the production of  $^1\text{O}_2$ , but also in the quenching of  $^1\text{O}_2$ . The increasing tendency of  $k_Q$  copies the increasing tendency of ground-state dipole moments  $\mu_r$ <sup>[11]</sup> although absolute correlation does not exist. Polarizability of the chromophore most likely contributes as another factor to CT-induced quenching of  $^1\text{O}_2$ . An opaque trend of  $k_Q$  behavior after the exchange of a CN group for an  $\text{NO}_2$  group in pairs **4–5** and **6–7** could be explained by different equilibrium between benzenoid and quinoid form of compound **6** in the ground state (values of  $\log \epsilon$  and  $f$  in Table 1).

**Self-sensitized photooxidation by  $^1\text{O}_2$ .** In many cases, CT quenching of  $^1\text{O}_2$  additionally competes with chemical reactions, which are often far from negligible.<sup>[52]</sup> To determine the fraction of chemical reaction with  $^1\text{O}_2$  in the overall quenching of  $^1\text{O}_2$ , we carried out a series of experiments in which the decrease in absorbance of **1–7** due to MB-generated  $^1\text{O}_2$  in the absence of any other quencher was monitored. According to the mechanism of photooxidation by  $^1\text{O}_2$ , the reaction rate at low concentration ( $\beta_r \gg [\text{C}]$ ) (assuming that  $^1\text{O}_2$  is constant) is given by the following equations:<sup>[33,34]</sup>

$$-\frac{d[\text{C}]}{dt} = \Phi_r I_a = \Phi_{^1\text{O}_2(\text{MB})} I_a \frac{[\text{C}]}{[\text{C}] + \beta_r} = k_f \frac{[\text{C}]}{[\text{C}] + \beta_r} = k_f \frac{[\text{C}]}{\beta_r} = k_f \frac{k_r}{k_d} [\text{C}] = k_r [\text{C}] [^1\text{O}_2] = K[\text{C}]. \quad (8)$$

The photofading rate constant  $K$  for the dyes was obtained

from the slope of the plot

$$\ln(A_0/A_t) = Kt, \quad (9)$$

where  $K = [\text{C}][^1\text{O}_2]$ .

Figure 4 shows the photostability of **4–7** in MeOH against  $^1\text{O}_2$  photooxidative attack. The linear relationships between  $\ln[A_0/A_t]$  and  $t$  indicate that these are first-order kinetics reactions. The slopes of the plots indicate that the photofading rate constant is the greatest for **4** and the smallest for **7** (Fig. 4B).

If the rate of  $^1\text{O}_2$  formation  $k_f$  is known, then we can calculate an objective value of the second-order rate constant  $k_r$  (or  $\beta_r$ ) for  $^1\text{O}_2$  photooxidative attack. The  $k_f$  value was obtained by multiplying the known value  $\Phi^1\text{O}_2$  for MB in MeOH by the value of  $I_a$  absorbed by this sensitizer. Results are summarized in Table 3.

Concentrations of chromophores **1–3** did not change after 2 h on irradiation at the same experimental conditions. This does not necessarily mean that molecules **1–3** do not react with  $^1\text{O}_2$ , but the second-order rate constant  $k_r$  should not exceed  $10^5 \text{ dm}^3 \text{ mol}^{-1} \text{ s}^{-1}$  ( $\beta_r \geq 0.1 \text{ mol dm}^{-3}$ ).

To determine the kinetic parameters of self-sensitized photooxidation due to  $^1\text{O}_2$  production and subsequent reaction between  $^1\text{O}_2$  and the sensitizer, we first calculated the time-dependent concentration values ( $c_{i+1}$ ) for this photodegradation pathway using the following equations:

$$c_{i+1} = c_i \exp\left(-\frac{\Phi_{^1\text{O}_2} I_a}{\beta_r} \Delta t\right), \quad I_{a_i} = I_{a_0} \frac{(1 - 10^{-\alpha c_i})}{(1 - 10^{-\alpha c_0})}, \quad (10)$$

$$i = 0, 1, 2, \dots, n; \Delta t = 50000\text{s}$$

and then subtracted the half-life times ( $t_{1/2(1\text{O}_2)}$ ) of the self-sensitized photooxygenation reaction and the times of degradation of 90% of the compound ( $t_{9/10(1\text{O}_2)}$ ) at these reaction from the corresponding graphs  $c_{i+1} = f(t_i)$  (Fig. 5) (coefficients  $\alpha$  were determined using OO SD 2000 spectrophotometer).

To compare the kinetic parameters of autooxidation by  $^1\text{O}_2$  for molecules with (**4–7**) and without (**1–3**) an acceptor group bonded to the heterocycle, the maximum values of  $k_r = 10^5 \text{ dm}^3 \text{ mol}^{-1} \text{ s}^{-1}$  ( $\beta_r \geq 0.1 \text{ mol dm}^{-3}$ , respectively) for all three chromophores **1–3** was taken. Results are summarized in Table 4. The obtained order of self-sensitized photodegradation for **1–3** coincides with

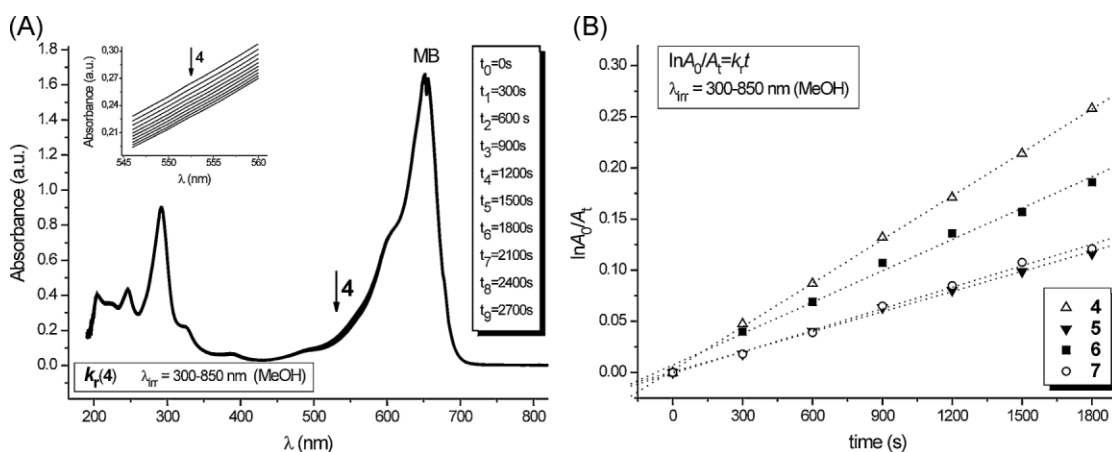


**Figure 4.** (A) Photodegradation of **4** in MeOH due to photooxidation by MB-generated  $^1\text{O}_2$  ( $\Phi^1\text{O}_2 = 0.50 \pm 0.01$ ,  $I_a = 4.5 \pm 0.5 \times 10^{-6} \text{ mol s}^{-1} \text{ dm}^{-3}$  for MB; color filter with transmittance  $>550 \text{ nm}$  was used to avoid direct photodegradation of **4**). (B) Photostability of MeOH solutions of **4–7** against  $^1\text{O}_2$  photooxidative attack (dotted lines, linear regression of experimental data)

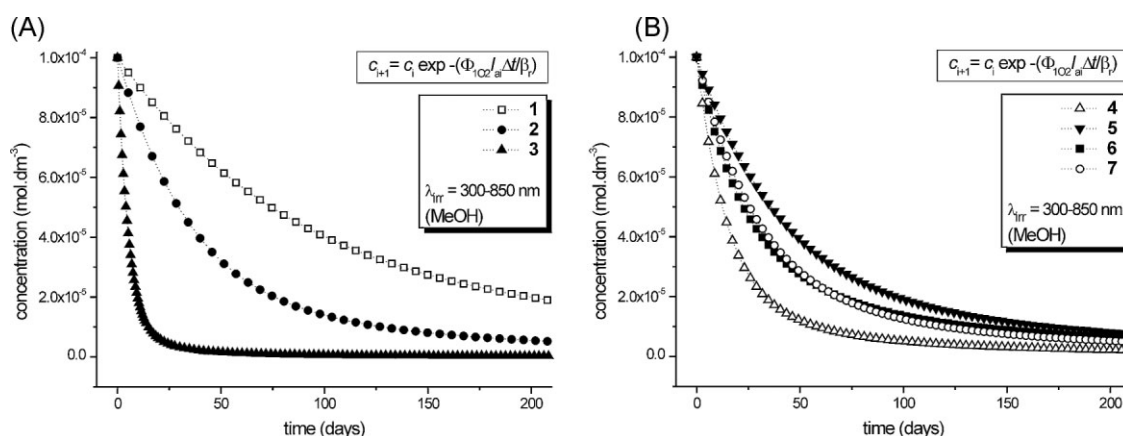


**Figure 5.** Calculated photodegradation curves of (A) **1–3** and (B) **4–7** in MeOH due to self-sensitized  $^1\text{O}_2$  photooxidative attack during irradiation at 300–850 nm (incident photon flux  $I_0 = 2.05 \times 10^{-5} \text{ mol s}^{-1} \text{ dm}^{-3}$ )

the order of photodegradation after 3 weeks of the exposure of solution of **1–3** ( $10^{-4} \text{ mol dm}^{-3}$ ) to daily sunlight. For a more accurate estimation of kinetic parameters describing this degradation pathway for **1–3**, further experiments with higher irradiation intensities and more effective sensitizer should be carried out.

The quantum yields ( $\Phi_{r(1O_2)}$ ) of these self-sensitized photodegradations were calculated according to:

$$\Phi_{r(1O_2)} = \frac{\Phi_{1O_2}}{\beta_r} [C]. \quad (11)$$

Values of  $\Phi_{r(1O_2)}$  are expressed as number  $\times [C]$  to point out their dependence on the concentration of the corresponding chromophore (Table 4). Times  $t_{1/2(1O_2)}$  and  $t_{9/10(1O_2)}$  are relatively high (except derivative **3** with  $t_{1/2(1O_2)} \sim 4$  days) and showed strong dependence on addition of an acceptor group to the heterocycle and the length of the conjugated bridge. Both structural changes decrease the overall photostability although the change is not so significant after the addition of an acceptor group to skeleton **2**. Self-sensitized photooxidation by  $^1\text{O}_2$  thus makes a slow parallel degradation pathway for irradiation at 300–850 nm and, albeit to the small  $\Phi$ , contributes with large fraction to the overall photodegradation of **4–7** (and probably also of **1–3**).

Exchange of the  $\text{NO}_2$  group for CN causes a large increase in the photostability of compound **5**, but had only a very small influence on the photostability of **7**. This difference could be most likely due to the equilibrium between resonance-forms of the ground state of compound **6**. The photostabilities of the chromophores can be placed in the order: **1** > **5** > **2** > **7** > **6** > **4** > **3**. It is apparent that a compromise should be made between an increase in NLO response and a decrease in photostability to enable a choice of NLO chromophores for practical applications.

Finally, the minimal overall degradation ( $\sim 1$ – $2\%$ ) due to *trans-cis* photoisomerization, the relatively low quantum yield for self-sensitized photooxidation by  $^1\text{O}_2$  as the main photodegradation pathway ( $0.014 \times [C]$  and  $0.012 \times [C]$ ) and the high  $\beta$  values ( $370 \times 10^{-30} \text{ esu}$  and  $184 \times 10^{-30} \text{ esu}$ ) mean that compounds **2** and **5** are promising for NLO applications. Compound **3**, albeit to very large value of  $\beta$ , is not a good candidate for practical NLO applications due to its poor photostability.

## CONCLUSIONS

In this paper, the photochemical stability of seven *D*– $\pi$ –*A* benzothiazolium salts as candidates for NLO chromophores were investigated. The studied compounds differed in length of conjugated bridge and presence (or absence) of an additional acceptor group ( $\text{NO}_2$  or CN) bound to position 6- of the *N*-methylbenzothiazolium moiety. The photoreaction quantum yield and the kinetic parameters were determined for existing photodegradation pathways on irradiation at 300–850 nm in MeOH. The most rapid reaction for any of the seven substrates is *trans-cis* photoisomerization, which leads to a photostationary state and contributes with a low percent ( $\sim 1$ – $7\%$  decrease of initial concentration) to the overall photodegradation. Photooxidation by  $^1\text{O}_2$  gives a second very slow parallel degradation pathway and, albeit to small values of  $\Phi$ , plays a dominant role in the photodegradation of **1–7**. Electron transfer (formation of a superoxide anion radical) and subsequent oxidation reactions (followed by various radical recombinations) or nucleophilic addition of  $\text{O}_2^-$  may contribute to the overall degradation of compound **4**. Both structural modifications increasing NLO response (extension of the conjugated bridge and an additional acceptor group bonded to the heterocycle) led to a decrease in photostability due to manifestation of the main photodegradation pathway (self-sensitized  $^1\text{O}_2$  photooxidative attack). From the values of the kinetic parameters of self-sensitized photooxidation by  $^1\text{O}_2$ , it can be concluded that a compromise should be made between an increasing NLO response and a decreasing photostability to enable a choice of NLO chromophores **1–7** for practical applications. The existence of photostationary states at  $\sim 1$ – $2\%$  degradation by photoisomerization and low photochemical quantum yield ( $\Phi = 0.014 \times [C]$  and  $0.012 \times [C]$ ) for the main photodegradation pathway, together with high  $\beta$  values mean that **2** and **5** are promising derivatives for NLO applications.

## Acknowledgements

This work was supported by the Slovak Research and Development Agency through APVV Grant No. 0259-07, by the Slovak Grant Agency for Science (VEGA No. 1/ 0639/08), UK Grant No. UK/229/2007, Grant Agency of the Czech Republic (GACR 203/08/

1157), and by the project MSM 0021620835 from the Ministry of Education, Youth, and Sports of the Czech Republic.

## REFERENCES

- [1] H. S. Nalwa, S. Miyata, *Nonlinear Optics of Organic Molecules and Polymers*, CRC Press, New York, **1997**.
- [2] S. R. Marder, B. Kippelen, A. K.-Y. Jen, N. Peyghambarian, *Nature* **1997**, *388*, 845.
- [3] Y. Shi, Ch. Zhang, H. Zhang, J. H. Bechtel, L. R. Dalton, B. H. Robinson, W. H. Steier, *Science* **2000**, *288*, 119.
- [4] L. R. Dalton, *Pure Appl. Chem.* **2004**, *76*, 1421.
- [5] L. R. Dalton, *Thin Solid Films* **2009**, *518*, 428.
- [6] D. R. Kanis, M. A. Ratner, T. J. Marks, *Chem. Rev.* **1994**, *94*, 195.
- [7] L. R. Dalton, Ch. Zhang, M.-Ch. Oh, H. Zhang, W. H. Steier, *Chem. Mater.* **2001**, *13*, 3043.
- [8] B. Murali, M. B. J. Diemeer, A. Driessen, M. Faccini, W. Verboom, D. N. Reinhoudt, A. Borreman, M. J. Gilde, *Proceedings Symposium IEEE/LEOS Benelux Chapter*, **2004**, Ghent.
- [9] E. M. Breitung, Ch.-F. Shu, J. R. McMahon, *J. Am. Chem. Soc.* **2000**, *122*, 1154.
- [10] P. Hrobárik, P. Zahradník, W. M. F. Fabian, *Phys. Chem. Chem. Phys.* **2004**, *6*, 495.
- [11] I. Sigmundová, P. Zahradník, D. Loos, *Collect. Czech. Chem. Commun.* **2007**, *72*, 1069.
- [12] M. H. Lu, Y. M. Liu, *Appl. Phys. B* **1992**, *354*, 288.
- [13] G. J. Ashwell, P. D. Jackson, W. A. Crossland, *Nature* **1994**, *368*, 438.
- [14] M. Zajac, P. Hrobárik, P. Magdolen, P. Foltínová, P. Zahradník, *Tetrahedron* **2008**, *64*, 10605.
- [15] P. Hrobárik, I. Sigmundová, P. Zahradník, *Synthesis* **2005**, *4*, 600.
- [16] R. Buffa, R. P. Zahradník, P. Foltínová, *Collect. Czech. Chem. Commun.* **2002**, *67*, 1820.
- [17] R. Buffa, R. P. Zahradník, P. Foltínová, *Heterocycl. Commun.* **2001**, *7*, 331.
- [18] B. J. Coe, J. A. Harris, J. J. Hall, B. S. Brunshwig, S.-T. Hung, W. Libaers, K. Clays, S. J. Coles, P. N. Horton, M. E. Light, M. B. Hursthouse, J. Garin, J. Orduna, *Chem. Mater.* **2006**, *18*, 5907.
- [19] A. Galvan-Gonzalez, M. Canva, G. I. Stegeman, R. Twieg, K. P. Chan, T. C. Kowalczyk, X. Q. Zhang, H. S. Lackritz, S. Marder, S. Thayumanavan, *Opt. Lett.* **2000**, *25*, 332.
- [20] A. Galvan-Gonzalez, K. D. Belfield, G. I. Stegeman, M. Canva, S. R. Marder, K. Staub, G. Levina, R. J. Twieg, *J. Appl. Phys.* **2003**, *94*, 756.
- [21] A. Galvan-Gonzalez, M. Canva, G. I. Stegeman, *Appl. Phys. Lett.* **1999**, *75*, 3306.
- [22] A. Galvan-Gonzalez, G. I. Stegeman, A. K.-Y. Jen, X. Wu, M. Canva, A. C. Kowalczyk, X. Q. Zhang, H. S. Lackritz, S. Marder, S. Thayumanavan, G. Levina, *J. Opt. Soc. Am. B* **2001**, *18*, 1846.
- [23] M. E. DeRosa, M. He, J. S. Cites, S. M. Garner, Y. R. Tang, *J. Phys. Chem. B* **2004**, *108*, 8725.
- [24] D. Rezzonico, M. Jazbinsek, P. Günter, Ch. Bosshard, D. H. Bale, Y. Liao, L. R. Dalton, P. J. Reid, *J. Opt. Soc. Am. B* **2007**, *24*, 2199.
- [25] C. C. Corredor, K. D. Belfield, M. V. Bondar, O. V. Przhonska, S. Yao, *J. Photochem. Photobiol. A: Chem.* **2006**, *184*, 105.
- [26] K. D. Belfield, M. V. Bondar, O. V. Przhonska, K. J. Schafer, *J. Photochem. Photobiol. A: Chem.* **2004**, *162*, 569.
- [27] A. Abboto, L. Beverina, G. Chirico, A. Facchetti, P. Ferruti, G. A. Pagani, *Synth. Metal.* **2003**, *139*, 629.
- [28] A. Gáplovský, Š. Toma, J. Donovalová, *J. Photochem. Photobiol. A: Chem.* **2007**, *191*, 162.
- [29] K. D. Belfield, C. C. Corredor, A. R. Morales, M. A. Dessources, F. E. Hernandez, *J. Fluorescence* **2006**, *16*, 105.
- [30] A. A. Krasnovsky, Jr., Ya. V. Roumbal, A. V. Ivanov, R. V. Ambartsumian, *Chem. Phys. Lett.* **2006**, *430*, 260.
- [31] H. Shiozaki, H. Nakazumi, Y. Takamura, T. Kitao, *Bull. Chem. Soc. Jpn* **1990**, *63*, 2653.
- [32] B. M. Monroe, *J. Phys. Chem.* **1977**, *81*, 1861.
- [33] P. Chen, S. Sun, Y. Hu, Z. Qian, D. Zheng, *Dyes Pigm.* **1999**, *41*, 227.
- [34] F. Wilkinson, W. P. Helman, A. B. Ross, *J. Phys. Chem. Ref. Data* **1995**, *24*, 663.
- [35] F. Amat-Guerri, M. M. C. López-González, R. Martínez-Utrilla, *J. Photochem. Photobiol. A: Chem.* **1990**, *53*, 199.
- [36] Y. Usui, M. Tsukada, H. Nakamura, *Bull. Chem. Soc. Jpn* **1978**, *51*, 379.
- [37] K. J. Reszka, M. Takayama, R. H. Sik, C. F. Chignell, Isao. Saito, *Photochem. Photobiol.* **2005**, *81*, 573.
- [38] S. Wei, J. Zhou, D. Huang, X. Wang, B. Zhang, J. Shen, *Dyes Pigm.* **2006**, *71*, 61.
- [39] R. Dedic, A. Svoboda, J. Pšenčík, J. Hála, *J. Mol. Struct.* **2003**, *301*, 651.
- [40] M. Dekhtyar, W. Rettig, M. Sczepan, *Phys. Chem. Chem. Phys.* **2000**, *2*, 1129.
- [41] S. E.-D. H. Etaiw, T. A. Fayed, N. Z. Saleh, *J. Photochem. Photobiol. A: Chem.* **2006**, *177*, 238.
- [42] W. Rettig, W. Baumann, in *Progress in Photochemistry and Photo-physics, Volume VI*, (Ed.: J. F. Rabek), CRC Press Inc., Boca Raton, Florida, **1992**, 100.
- [43] X. Guo, S. Wang, A. Xia, H. Su, *J. Phys. Chem. A* **2007**, *111*, 5800.
- [44] S. N. Batchelor, D. Carr, C. E. Coleman, L. Fairclough, A. Jarvis, *Dyes Pigm.* **2003**, *59*, 269.
- [45] X. Chen, X. Peng, A. Cui, B. Wang, L. Wang, R. Zhang, *J. Photochem. Photobiol. A: Chem.* **2006**, *181*, 79.
- [46] C. B. Nielsen, M. Johnsen, J. Arnbjerg, M. Pittelkow, S. P. McIlroy, P. R. Ogilby, M. Jørgensen, *J. Org. Chem.* **2005**, *70*, 7065.
- [47] S. P. McIlroy, E. Cló, L. Nikolajsen, P. K. Frederiksen, C. B. Nielsen, K. V. Mikkelsen, K. V. Gothelf, P. R. Ogilby, *J. Org. Chem.* **2005**, *70*, 1134.
- [48] C. B. Nielsen, J. Arnbjerg, M. Johnsen, M. Jørgensen, P. R. Ogilby, *J. Org. Chem.* **2009**, *74*, 9094.
- [49] M. Bennati, K. Németh, P. R. Surján, M. Mehring, *J. Chem. Phys.* **1996**, *105*, 4441.
- [50] D. Beljonne, J. Cornil, R. H. Friend, R. A. J. Janssen, J. L. Brédas, *J. Am. Chem. Soc.* **1996**, *118*, 6453.
- [51] E. Peeters, A. M. Ramos, S. C. J. Meskers, R. A. J. Janssen, *J. Chem. Phys.* **2000**, *112*, 9445.
- [52] C. Schweitzer, R. Schmidt, *Chem. Rev.* **2003**, *103*, 1685.
- [53] J. R. Kanofsky, P. D. Sima, *Photochem. Photobiol.* **2000**, *71*, 361.